Folding thermodynamics and kinetics of the leucine-rich repeat domain of the virulence factor Internalin B

NAOMI COURTEMANCHE AND DOUG BARRICK

T.C. Jenkins Department of Biophysics, The Johns Hopkins University, Baltimore, Maryland 21218, USA

(RECEIVED August 8, 2007; FINAL REVISION October 5, 2007; ACCEPTED October 8, 2007)

Abstract

Although the folding of α-helical repeat proteins has been well characterized, much less is known about the folding of repeat proteins containing β-sheets. Here we investigate the folding thermodynamics and kinetics of the leucine-rich repeat (LRR) domain of Internalin B (InlB), an extracellular virulence factor from the bacterium *Lysteria monocytogenes*. This domain contains seven tandem leucine-rich repeats, of which each contribute a single β-strand that forms a continuous β-sheet with neighboring repeats, and an N-terminal α-helical capping motif. Despite its modular structure, InlB folds in an equilibrium two-state manner, as reflected by the identical thermodynamic parameters obtained by monitoring its sigmoidal urea-induced unfolding transition by different spectroscopic probes. Although equilibrium two-state folding is common in α-helical repeat proteins, to date, InlB is the only β-sheet-containing repeat protein for which this behavior is observed. Surprisingly, unlike other repeat proteins exhibiting equilibrium two-state folding, InlB also folds by a simple two-state kinetic mechanism lacking intermediates, aside from the effects of prolyl isomerization on the denatured state. However, like other repeat proteins, InlB also folds significantly more slowly than expected from contact order. When plotted against urea, the rate constants for the fast refolding and single unfolding phases constitute a linear chevron that, when fitted with a kinetic two-state model, yields thermodynamic parameters matching those observed for equilibrium folding. Based on these kinetic parameters, the transition state is estimated to comprise 40% of the total surface area buried upon folding, indicating that a large fraction of the native contacts are formed in the rate-limiting step to folding.

Keywords: repeat protein; leucine-rich repeat; protein folding; kinetics

Supplemental material: see www.proteinscience.org

Repeat proteins, which are composed of linear tandem arrays of repeated secondary structural elements, make excellent model systems for folding studies. Repeat proteins have the same secondary structural elements and close packing interactions as globular proteins; however, the modular, linear structure of repeat proteins gives rise to a local topology and low contact order that permits the study of the limits of folding cooperativity. Moreover, the structural redundancy of repeat proteins facilitates a comparison of the energy distribution and kinetic pathway selection among similar structural elements (Kloss et al. 2007). Recent studies have elucidated the folding pathways of several naturally occurring α-helical repeat proteins (Tang et al. 1999; Zeeb et al. 2002; Bradley and Barrick 2006; Lowe and Itzhaki 2007b). Although most helical repeat proteins fold via an equilibrium, two-state mechanism, the kinetic pathways of these proteins are complex, often involving one or more on-pathway intermediates (Kloss et al. 2007).

Compared to α-helical repeat proteins, the folding of repeat proteins with β-sheet structure has not been studied extensively (Kamen et al. 2000; Kamen and Woody 2001;

Reprint requests to: Doug Barrick, T.C. Jenkins Department of Biophysics, The Johns Hopkins University, 3400 North Charles Street, Baltimore, MD 21218, USA; e-mail: barrick@jhu.edu, fax: (410) 516-4118.

Article and publication are at http://www.proteinscience.org/cgi/doi/10.1110/ps.073166608.

Junker et al. 2006). Here we investigate the equilibrium and kinetic folding mechanism of the leucine-rich repeat (LRR) domain of Internalin B (InlB), a virulence factor from *Listeria monocytogenes*. The LRR domain of InlB is composed of a linear array of seven tandemly repeated LRR motifs of 22 residues, each made up of a short β-strand, followed by a tight turn and a 3_{10} helix (Fig. 1). Consecutive repeats are connected by a turn and stack linearly. The N terminus of the LRR array is capped by a 40-residue α-helical motif; the C terminus is capped by a single β-strand, which continues the LRR β-sheet (Marino et al. 1999).[1] This modular architecture results in a local topology that is free of the long-range contacts that typify most globular proteins.

Given its size, architecture, and spectroscopic properties, InlB is well suited for studies of the cooperativity and kinetics of folding of LRR domains. In a previous study, Freiberg et al. (2004) found a single coincident folding transition by circular dichroism- (CD) and fluorescence-monitored chemical denaturation. However, the unfolding transition was unusually steep and was found to become even steeper upon addition of Ca^{2+}. In combination with crystallographic evidence for Ca^{2+}-mediated interactions, the high and variable steepness of the equilibrium unfolding transition observed by Freiberg et al. (2004) suggests that folding may be coupled to native-state association.

To better characterize the equilibrium folding mechanism of monomeric InlB and to characterize the kinetic mechanism of folding, we measured folding and unfolding of InlB using multiple spectroscopic probes, both at equilibrium and in kinetic studies. We have measured equilibrium unfolding transitions by far-UV CD in the β-sheet region, tryptophan fluorescence, and near-UV CD using a multi-wavelength analysis. We have also investigated the potential for oligomer formation using analytical ultracentrifugation. These equilibrium spectroscopic and hydrodynamic studies allow us to examine the cooperativitiy of folding of a monomeric species, to assess whether the modular structure of this domain results in modular thermodynamics. The kinetic studies permit us to analyze the mechanism of folding, test for kinetic intermediates, evaluate the influence of the local topology on folding rate, and begin to investigate the structural and energetic properties of the transition state ensemble. This study lays the foundation for residue-specific analysis of LRR folding.

Results

Urea-induced equilibrium denaturation of Internalin B

To determine the stability and the extent of folding cooperativity of InlB, we monitored urea-induced denaturation by CD at 217 nm, tryptophan fluorescence, and near-UV CD. The primary contribution of the CD signal at 217 nm is β-sheet structure, which is distributed across the entire LRR domain. The primary contribution of fluorescence change upon unfolding is a single tryptophan residue located in the third repeat of the LRR domain of InlB (Fig. 1). The primary contributions to CD in the near-UV region, which reflects the amount of rigid tertiary structure in the protein, are specific side-chain interactions involving the aromatic residues (1 trp, 3 tyr) (see Supplemental Fig. S1 for full far- and near-UV CD spectra). Taken together, these three spectroscopic probes allow a comparison of local and global unfolding of InlB.

The CD at 217 nm and fluorescence-monitored urea denaturation curves are sigmoidal, have well-defined baselines, and can each be described by an equilibrium two-state model in which unfolding free energy is linearly dependent on denaturant concentration (Fig. 2A). The fitted thermodynamic parameters from far-UV CD and fluorescence are the same, within error. The near-UV CD-monitored denaturation also captures a sharp unfolding transition. Because

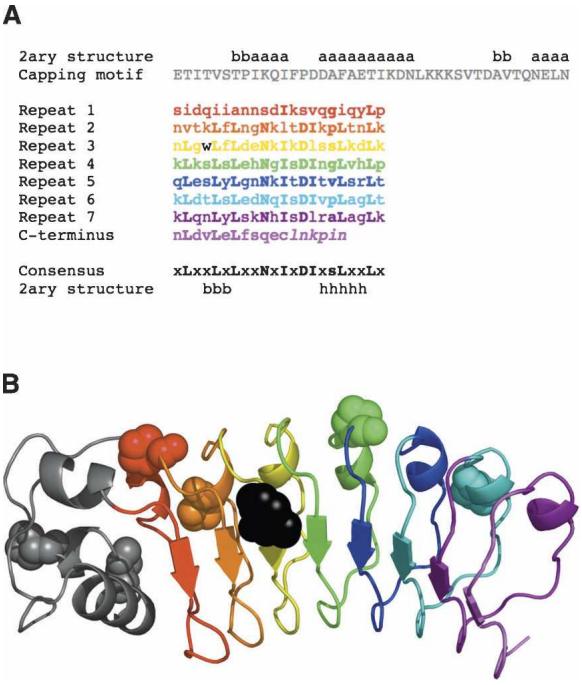

Figure 1. Sequence and ribbon diagram of the seven leucine-rich repeats and α-helical capping motif (gray) of InlB. (*A*) Sequence of the LRR domain of InlB studied here. Secondary structure assignments (x = any residue, a = α-helix, b = β-strand, h = 3_{10} helix, s = small residue) are taken from Marino et al. (1999). The single cysteine, located in the C-terminal β-strand, was replaced with a serine. Residues not visible in the crystal structure are shown in italics. (*B*) Ribbon diagram of the crystal structure of InlB (Marino et al. 1999). The six *trans*-proline residues are shown in CPK representation. The single tryptophan, located in the third leucine-rich repeat, is shown in black. Panel *B* was generated using PyMOL (DeLano Scientific).

[1]In addition, in the full-length protein, the LRR domain is stabilized by a C-terminal immunoglobulin-like domain (Freiberg et al. 2004).

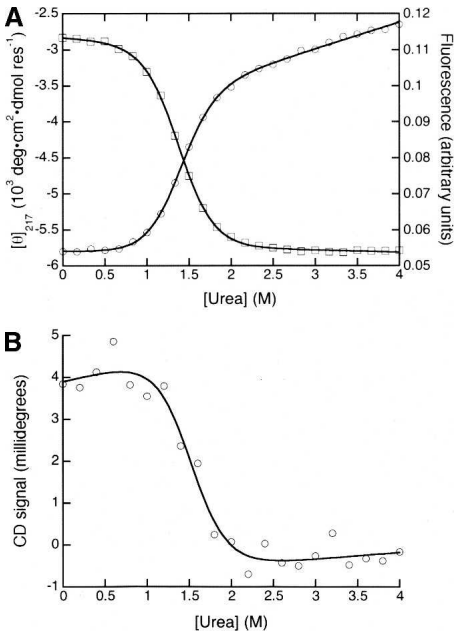

Figure 2. Urea-induced equilibrium unfolding of InlB. (*A*) Denaturation curves were monitored by CD at 217 nm (circles) and tryptophan fluorescence (squares), and fit with a two-state model using the linear extrapolation method. (*B*) Urea-induced unfolding of InlB monitored by near-UV CD. Near-UV spectra were integrated from 260 to 287 nm at each urea concentration (circles) and fit with a two-state model (solid line). Conditions: 3 μM protein, 150 mM NaCl, 25 mM Tris (pH 8.0), 25°C.

there is substantial noise at each wavelength in the near-UV region, we collected full near-UV CD spectra as a function of urea concentration and globally fitted these spectra from 260 to 287 nm using a two-state model. As an independent means of analyzing the data, we integrated the near-UV spectra over the same wavelength range and fitted the resulting transition to a two-state model (Fig. 2B). Thermodynamic unfolding parameters fitted from the near-UV CD spectra using both methods of analysis match those determined by CD at 217 nm and by fluorescence (Table 1). This close agreement supports an equilibrium two-state folding pathway.

The steepness of the unfolding transition permits a quantitative measure, through the *m*-value, of the cooperativity of unfolding. An observed linear relationship between the steepness of two-state unfolding transitions and chain length predicts an *m*-value of 2.45 $kcal.mol^{-1}.M^{-1}$ for InlB, assuming the helical capping motif and LRR domain are thermodynamically coupled (Myers et al. 1995). The close agreement between this predicted *m*-value and the *m*-values observed by monitoring equilibrium unfolding transitions by fluorescence, CD (217 nm), and near-UV CD (Table 1) further suggests that the seven LRRs unfold in a concerted reaction that includes the α-helical capping motif.

The *m*-values and free energies of unfolding that we determined from our equilibrium denaturation experiments are ~30% smaller than those previously published (Freiberg et al. 2004). One possible explanation for this discrepancy is that the previous measurements were made at lower ionic strength, temperature, and pH.[2] To explore this possibility, we monitored equilibrium denaturation in solution conditions identical to those used by Freiberg et al. (2004). Regardless of conditions, we obtain the same fitted thermodynamic parameters (data not shown). Therefore, the difference between the thermodynamic parameters we measured and those previously published do not appear to result from a difference in ionic strength or pH.

Association state of Internalin B

A second possible explanation for the higher *m*-value and free energy of unfolding reported by Freiberg et al. (2004) is self-association of folded InlB. The crystal structure of InlB reveals a large interface for potential self-association; this interface includes binding sites for two Ca^{2+} ions (Marino et al. 1999). In support of native-state association via this interface and its contribution to the anomalous *m*-value, Freiberg et al. (2004) found that the *m*-value further increases in the presence of Ca^{2+}.

To investigate the state of association of InlB under the conditions used here and to examine the effects of Ca^{2+} on potential association, we performed sedimentation equilibrium analytical ultracentrifugation experiments of InlB in various concentrations of Ca^{2+}. We find that a model involving a single, monomeric species is adequate to describe the sedimentation equilibrium of InlB both in the absence and presence of 50 mM Ca^{2+} (Fig. 3). The residuals from these monomeric fits are small and are not significantly decreased by the inclusion of a dimeric species. The molecular weights of the single species in these fits match the calculated molecular weight of monomeric InlB, suggesting that the protein is monomeric under these conditions (Table 2). This finding simplifies the analysis of both equilibrium and kinetic folding data, although it does not explain the higher cooperativity seen by Freiberg et al. (2004).

Recently, a second mode of self-association of the LRR domain of InlB has been identified (Banerjee et al. 2004). This mode of asocciation is mediated by disulfide bond formation involving the single cysteine located at the C terminus of the LRR domain. This cysteine is present in the construct studied by Freiberg et al. (2004); however, we have replaced it with a serine to promote long-term stability and avoid intermolecular association (see

[2]Unfolding transitions reported by Freiberg et al. (2004) were performed in 40 mM Tris-HCl, 1 mM EDTA (pH 7.0), 20°C; here we use 150 mM NaCl, 25 mM Tris-HCl (pH 8.0), 25°C.

Table 1. *Thermodynamic parameters determined from equilibrium and kinetic studies*

	Equilibrium studies				Kinetic studies[a]	
	Fluorescence[b]	CD_{217nm}[b]	$CD_{Near\text{-}UV}$[c]	$CD_{Near\text{-}UV}$[d]	Fluorescence + CD_{217nm}	Fluorescence alone
$\Delta G^{\circ}_{u,H_2O}$ (kcal.mol)	3.94 ± 0.07	3.89 ± 0.06	4.11	3.82	3.62	3.87
m-value (kcal.mol^{-1}.M^{-1})	2.83 ± 0.01	2.77 ± 0.04	2.72	2.54	2.43	2.50
C_m (M)	1.39 ± 0.08	1.40 ± 0.10	1.51	1.50	1.49	1.55
β_T	N/A	N/A	N/A	N/A	0.40	0.38

[a] Parameters estimated by fitting a kinetic two-state model (Equation 6) to the rate constants for the major refolding phase and the unfolding phase as a function of urea. Parameters were corrected for the contribution of prolyl isomerization (see footnote 3 in text).
[b] Parameters estimated by fitting the linear free energy equation (Equation 2) to urea-induced unfolding transitions. Errors in thermodynamic parameters determined by equilibrium studies are standard errors of the mean.
[c] Parameters are from fitting Equation 2 to the integrated near-UV CD intensity.
[d] Parameters are from global analysis of near-UV spectra as a function of urea concentration.
Conditions: 150 mM NaCl, 25 mM Tris-HCl (pH 8.0), 25°C.

Materials and Methods). The elimination of this dimer-promoting residue may account for the differences between the thermodynamic parameters we report and those published by Freiberg et al. (2004).

Refolding and unfolding kinetics of Internalin B

The equilibrium two-state folding and monomeric association state make InlB an ideal candidate for kinetic studies. To gain insight into the kinetic folding pathway of InlB, we monitored refolding and unfolding in various concentrations of urea both by tryptophan fluorescence and by CD at 217 nm. We found fluorescence-monitored refolding curves to be multiphasic, as evidenced by the nonrandom residuals generated by fitting a single exponential (Equation 6, $i = 1$) to the data (black curve, Fig. 4A). In contrast, refolding curves are well-fitted by a double exponential (Equation 6, $i = 2$; red curve, Fig. 4A), resulting in much smaller and more randomly distributed residuals (top panel, Fig. 4A). Higher order exponential fits (Equation 6, $i = 3$ or more) do not significantly improve χ_r^2 (data not shown). At 0.18 M urea, the fast refolding phase is the dominant phase, with an amplitude of ~70% of the total observed signal change (Table 3, see below).

The CD-detected refolding kinetics are noisier than those collected by fluorescence. As a result, the residuals from a single-exponential fit to stopped-flow CD data (black curve, Fig. 5A) are substantially larger than those from fluorescence, and deviation from single-exponential decay is less obvious than for fluorescence (Fig. 4A). However, at early refolding times, a clear, systematic deviation can be seen between the stopped-flow CD data and a fitted single-exponential decay. This deviation is eliminated when a second exponential phase is included (red curve, Fig. 5A), and χ_r^2 decreases significantly.

Although these results provide clear indication that, like fluorescence-monitored refolding, the CD-monitored refolding transitions are best described by a double exponential, the low signal-to-noise ratio prevents an accurate determination of rate constants and amplitudes of both phases. To test whether the rate constant of the major CD-detected refolding phase matches that from fluorescence, CD-detected refolding curves were fitted with double-exponential functions in which the rate constant for the slower phase and the relative amplitudes (k_2, A_1, and A_2, Equation 6) were held fixed at the values extracted from the fluorescence data at each urea concentration. With these constraints, the rate constant for the fast folding phase (k_1) of InlB determined by CD is within error of that determined by fluorescence (Table 3).

In contrast to refolding, the unfolding of InlB appears to be a single-exponential process both by fluorescence and CD. For both probes, unfolding curves are well described by a single exponential (black curves, Figs. 4B, 5B), resulting in randomly distributed residuals (top panels, Figs. 4B, 5B). Inclusion of a second exponential

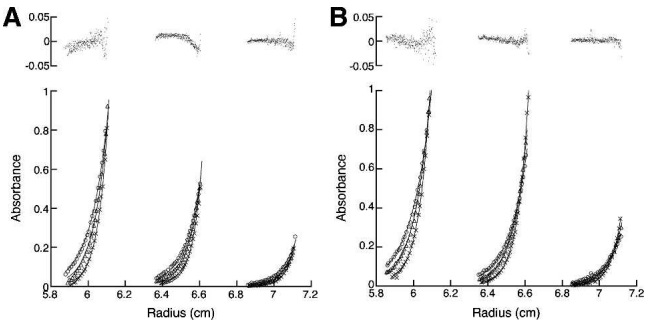

Figure 3. Equilibrium analytical ultracentrifugation of InlB. Absorbance at 280 nm versus radial position at three different protein concentrations and rotor speeds in the presence of (*A*) 0 mM and (*B*) 50 mM Ca^{2+}. Loading concentrations of InlB were 44 (*inner* sector), 26 (*middle* sector), and 9 μM (*outer* sector). Symbols indicate speeds of 23 (circles), 26 (triangles), and 30 krpm (X's). Solid lines are the result of simultaneous fitting of an ideal single-species model to the data. *Upper* panels show combined residuals for all three speeds and concentrations.

Table 2. *Molecular weights of InlB in varying concentrations of Ca^{2+} determined by analytical ultracentrifugation*

$[Ca^{2+}]$ (mM)	Molecular weight (Da)[a]	Standard deviation[b]
0	31,065	1.27×10^{-2}
10	29,883	1.24×10^{-2}
50	27,101	8.17×10^{-3}
Predicted from sequence	26,166	N/A

All measurements made in 150 mM NaCl, 25 mM Tris (pH 8.0), 25°C.
[a] Determined by global fitting of data from multiple protein concentrations and rotor speeds, as described in Materials and Methods.
[b] Standard deviation is the global root mean square deviation for the fit.

does not result in a significant improvement in χ_r^2 (data not shown).

The role of prolyl isomerization in the slow refolding phase

InlB contains six *trans* proline residues, two in the helical capping motif and four distributed among the LRR repeats (Marino et al. 1999; Fig. 1). Two observations suggest that these six proline residues give rise to the slow kinetic refolding phase. First, the rate constant for the slow refolding phase (0.09 s^{-1} in 0.18 M urea; Table 3) is within the range reported for prolyl isomerization in unstructured peptides (0.01–0.1 s^{-1}) (Brandts et al. 1975). Second, the rate constant for the slow phase has a shallow urea dependence (Fig. 7A, below), as are prolyl isomerization-limited refolding phases in other proteins (Schmid 1992).

To further test whether these proline residues give rise to the slow refolding phase, we monitored the effects of cyclophilin, a peptidyl-prolyl isomerase, on the major and minor refolding rates of InlB by fluorescence. Cyclophilin increases the rate constant of the slow refolding phase by nearly fourfold, reaching a plateau at ~2 μM cyclophilin (Fig. 6). Although the rate constant of the fast refolding phase appears to increase slightly in the presence of concentrations of cyclophilin above 2.5 μM, this may be a result of the convergence of the rates of the slow and fast phases at high concentrations of cyclophilin. Indeed, kinetic refolding curves are fitted equally well, based on χ_r^2 values, by a double exponential in which the rate constant of the fast phase is held fixed at the value determined in the absence of cyclophilin, whereupon the rate constant of the slow phase increases with cyclophilin in the same manner as when both rate constants are allowed to vary (not shown).

Urea dependence of refolding and unfolding rates of Internalin B

For proteins that fold by simple two-state kinetic mechanisms, the rate constants for folding and unfolding show log-linear dependences on urea concentrations, and together constitute a simple V-shaped ''chevron'' plot. In contrast, proteins that fold via more complicated mechanisms often display curvature in the folding or unfolding limb of their chevron plots (Baldwin 1996). For InlB, the fast refolding phase and the unfolding phase constitute a linear chevron plot (Fig. 7A), suggesting a simple kinetic two-state model. Both the fast refolding phase and unfolding phase have a steep urea dependence. In contrast, the rate constant for the slow refolding phase is much less sensitive to urea concentration. A kinetic two-state model (Equation 7) fits the fluorescence rate constants well (solid line, Fig. 7A) and yields rates of folding and unfolding in water (k_f and k_u, respectively) of 1.2 s^{-1} and 1.3 $\times$ 10^{-3} s^{-1}, respectively. Although the deviations between the rates determined by the two probes is greater than their associated errors at each urea concentration, similar rate constants are obtained when the fluorescence and CD rate constants are globally fitted to a kinetic two-state model (1.1 s^{-1} and 1.7 $\times$ 10^{-3} s^{-1},

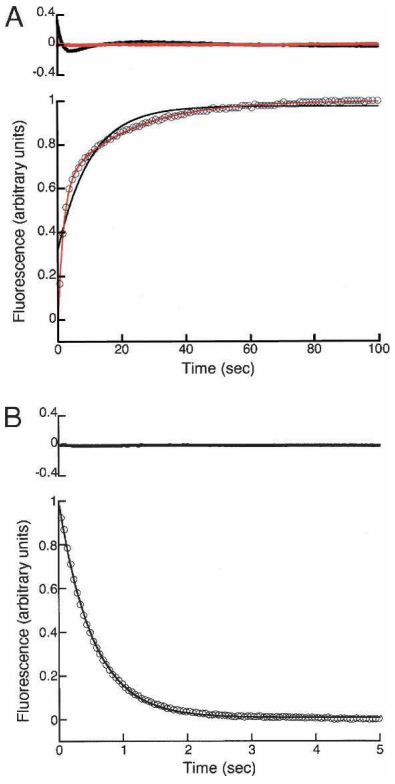

Figure 4. Fluorescence-detected refolding and unfolding of InlB. (*A*) Refolding was initiated by rapid dilution of urea from 3 M to 0.18 M. Refolding data (circles) were fitted with single- and double-exponential functions (black and red solid lines, respectively) according to Equation 6. (*B*) Unfolding was initiated by rapid addition of urea from 0 M to 2.95 M. Unfolding data (circles) were fitted with a single-exponential function (black line) according to Equation 6. *Upper* panels show residuals for each fit. For clarity, only every 10th data point is shown in each panel.

Table 3. *Fitted parameters for fluorescence- and CD-detected refolding and unfolding of InlB*

	Refolding					Unfolding	
	k_1 (s^{-1})	A_1	k_2 (s^{-1})	A_2	χ_r^{2a}	k_1 (s^{-1})	χ_r^{2a}
Fluorescence[b]	0.870 ± 0.009	0.680 ± 0.001	0.092 ± 0.002	0.320 ± 0.001	2.0×10^{-5}	2.060 ± 0.011	1.1×10^{-3}
CD_{217nm}[c]	0.900	Fixed at 0.680	Fixed at 0.092	Fixed at 0.320	1.2×10^{-3}	1.900	2.9×10^{-2}

Refolding was to final urea concentrations of 0.18 M and 0.2 M for experiments monitored by fluorescence and CD, respectively. Unfolding was to final urea concentrations of 2.95 and 3.0 M urea for experiments monitored by fluorescence and CD, respectively. k_1 and k_2 refer to the major and minor phases (largest and smallest relative amplitudes), respectively. Amplitudes are calculated relative to the difference between the denatured (starting) and native (equilibrium) signals.

[a] The reduced chi-squared statistic is defined as: $\chi_r^2 = \frac{1}{d}\sum_{i=1}^{n}(Y_i - f(t_i))^2$ where Y_i and $f(t_i)$ are the observed and predicted spectroscopic signals at time t_i and d is the number of degrees of freedom remaining after fitting.

[b] Errors in fluorescence-monitored rate constants and amplitudes are standard errors of the mean from four separately fitted progress curves. χ_r^2 values for fluorescence-detected refolding and unfolding are evaluated over 25 and 5 sec of data, respectively.

[c] χ_r^2 values for CD-detected refolding and unfolding are evaluated over 25 and 5 sec of data, respectively.

Conditions: 150 mM NaCl, 25 mM Tris HCl (pH 8.0), 25°C.

respectively; Table 3), suggesting that the fluorescence and CD describe the same folding and unfolding transitions. The amplitudes of the major and minor refolding phases are also sensitive to urea concentration (Fig. 7B). At low urea concentrations, the fast refolding phase is dominant; however, its amplitude decreases, at the expense of the slow refolding phase, as urea concentration increases. The two amplitudes cross at ~1 M, above which the slow refolding phase becomes dominant.

A test for burst-phase intermediates

The linear chevron described by the major refolding and unfolding rate constants of InlB is suggestive of two-state kinetics. However, it is possible for a rapidly forming refolding intermediate to be populated within the dead time of the stopped flow (Kuwajima 1989; Kuwajima et al. 1991; Mann and Matthews 1993; Shastry and Roder 1998; Myers and Oas 2002). To test for such an intermediate, we compared initial values observed in stopped-flow fluorescence refolding experiments with values expected for the denatured and native states of InlB (Y_D and Y_N, respectively). At each urea concentration, Y_D values were estimated from a linear extrapolation of fluorescence signals arising from denatured protein in high concentrations of urea. Y_N values were measured by directly equilibrating native protein at each urea concentration. Fractional burst-phase changes (f_B) were calculated as

$$f_B = \frac{Y_0 - Y_D}{Y_N - Y_D} \quad (1)$$

where Y_0 is the starting fluorescence signal in a stopped-flow refolding trace.

At all denaturant concentrations, the burst-phase amplitudes detected by fluorescence are small (Fig. 8). At the lowest urea concentration we examined (0.27 M), the burst-phase amplitude was 14% of the expected signal (that is, 86% of the expected total amplitude is observed). By 1 M urea, the burst-phase amplitude decreases to 5%. The linear decrease in burst-phase signal for InlB differs from the sigmoidal burst phases of several proteins with rapid refolding intermediates (Kuwajima 1989; Kuwajima et al. 1991; Mann and Matthews 1993; Shastry and Roder 1998; Myers and Oas 2002). Taken together, the small burst-phase signal and linear chevron support direct refolding from the denatured state.

Discussion

Leucine-rich repeat-containing proteins such as InlB share several characteristics that make them interesting targets of folding studies. Free of the three-dimensional packing constraints that typify globular proteins, these elongated proteins can be quite large and thus may be expected to fold via complicated pathways involving both equilibrium and kinetic intermediates. Most LRR domains are also flanked by helical capping motifs at either or both termini (Ceulemans et al. 1999; Marino et al. 1999; Wu et al. 2000; Huyton and Wolberger 2007; Kim et al. 2007); in addition to enhancing the solubility of LRR domains, these caps may also contribute to the folding and possible self-association. The goal of this study is to determine and quantify the equilibrium and kinetic folding mechanisms of InlB, to gain insight into cooperativity, to test for potential folding intermediates, and to gain insight into the rate-limiting steps and transition state structure that control the folding of these unique LRR architectures.

Two-state equilibrium folding of InlB

The LRR domain of InlB folds in an equilibrium two-state manner, as evidenced by the coincident all-or-none

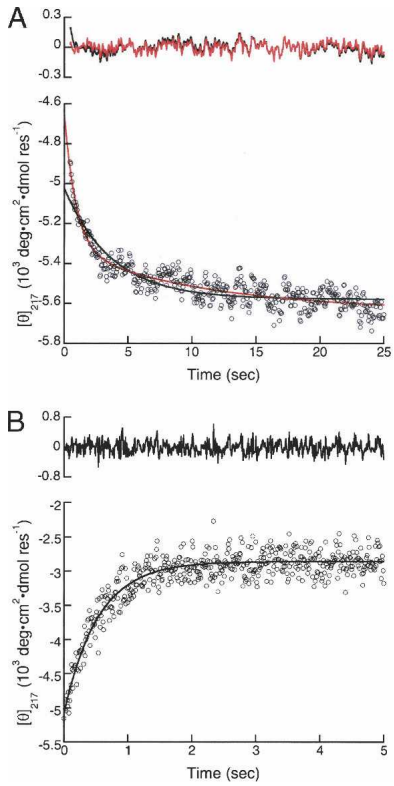

Figure 5. CD-detected refolding and unfolding of InlB. (*A*) Refolding was initiated by rapid dilution of urea from 3 M to 0.2 M. Data (circles) were fitted with single- and double-exponential fits (black and red solid lines, respectively). For the double-exponential fit, the slow rate and the relative amplitudes of the fast and slow phases were fixed at the values determined by fitting the tryptophan fluorescence-monitored kinetics at the same denaturant concentration. (*B*) Unfolding was initiated by rapid addition of urea from 0 M to 3.0 M. Data (circles) were fitted with a single-exponential function (black line) according to Equation 6. *Upper* panels show residuals for each fit.

transitions and the agreement between the thermodynamic parameters extracted from our equilibrium denaturation experiments monitored by different spectroscopic probes (far-UV CD, near-UV CD, and tryptophan fluorescence). The finding here that InlB folds by an equilibrium two-state mechanism is consistent with the finding of Freiberg et al. (2004), who reported identical far-UV CD- and tryptophan fluorescence-detected unfolding curves.

The fitted thermodynamic parameters reported by Freiberg et al. (2004) and the *m*-value in particular are significantly larger than those extracted from our equilibrium folding studies. This discrepancy does not result from a difference in solution conditions. Whereas the increased *m*-value observed by Freiberg et al. (2004) is suggestive of noncovalent self-association, we have found that InlB is monomeric in solution and that Ca^{2+} does not mediate association. It is possible that the discrepancy results from the single cysteine residue in the construct of Freiberg et al. (2004) (which we substituted with a serine residue in our construct), which has recently been implicated in self-association (Banerjee et al. 2004). Regardless of the source of discrepancy, confirmation that the native state of the InlB construct used in the present study is monomeric simplifies studies of both the thermodynamics and kinetics of folding.

The contribution of proline residues to refolding heterogeneity

InlB shows two well-resolved kinetic refolding phases. Several characteristics of the slow refolding phase are consistent with prolyl isomerization. First, the rate associated with the slow phase falls within the expected range for prolyl isomerization (0.01–0.1 s^{-1}). Second, the rate of this phase is insensitive to urea concentration, while its associated amplitude increases as a function of urea concentration (Fig. 7A,B), as is often seen when folding is coupled to prolyl isomerization (Kiefhaber et al. 1992; Bradley and Barrick 2005; Mello et al. 2005). In addition, peptidyl-prolyl isomerase increases the rate of the minor phase while the rate of the major phase remains constant (Fig. 6). The amplitude associated with the slow refolding phase matches the amplitude of the slow phase of the Notch ankyrin repeat domain, which contains approximately the same number of proline residues (Bradley and Barrick 2005). Taken together, these observations suggest that the refolding heterogeneity arises from the *cis–trans* isomerization reactions of proline residues in the denatured state of InlB. Thus, the fast refolding phase can be considered to reflect the barrier (or barriers) to folding, independent of prolyl isomerization.

Two-state kinetic folding of InlB

The urea dependences of the rates of the fast refolding and unfolding phases give rise to a linear chevron (Fig. 7A).

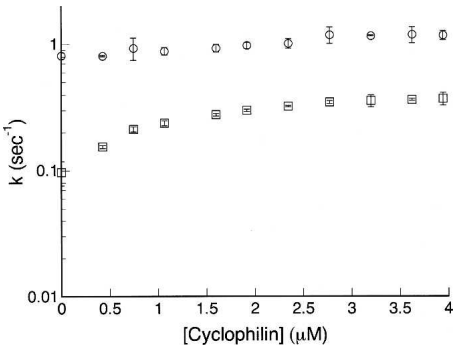

Figure 6. The effect of cyclophilin on refolding rate constants of InlB. Denatured InlB was refolded by rapid dilution from 3 M into 0.27 M urea and varying concentrations of cyclophilin. Refolding rate constants (fast phase, circles; slow phase, squares) were determined by fitting with a double-exponential model.

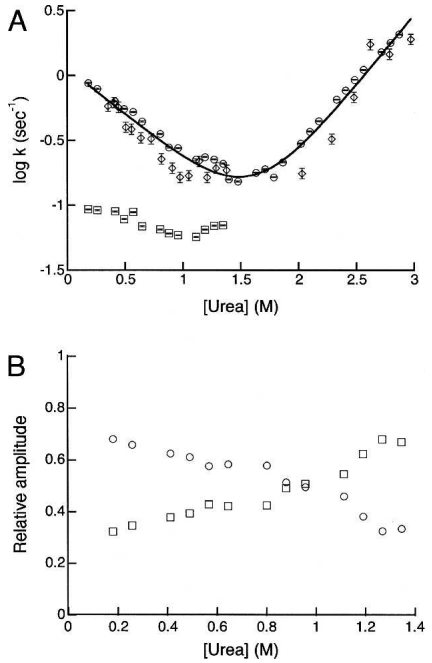

Figure 7. Chevron plot of InlB. (*A*) Folding and unfolding monitored by tryptophan fluorescence (fast phase, circles; slow phase, squares) and by CD at 217 nm (fast phase, diamonds). The fast phases detected by fluorescence and CD data were fitted simultaneously with a kinetic two-state model (black line), according to Equation 7. Fitting the fluorescence data alone yields similar values of k_{f,H_2O} and k_{u,H_2O}. Error bars are standard deviations on the mean of rate constants from five independent progress curves. (*B*) Relative amplitudes of the fast (circles) and slow (squares) refolding phases of InlB, determined by fitting fluorescence-monitored refolding data with a double-exponential function.

This chevron is consistent with a simple kinetic model where only two states, the native and denatured states, are populated upon folding:

$$D \rightleftharpoons N$$

Here, D represents a denatured state ensemble composed of denatured proteins with all kinetically limiting proline residues in the *trans* configuration. However, a linear chevron may also result in a three-state mechanism in which the denatured state immediately and quantitatively converts to a kinetic intermediate during the dead time of the reaction at all denaturant concentrations where refolding is observed:

$$D \rightarrow I \rightleftharpoons N$$

In such cases the observed refolding kinetics monitors the formation of N from I, rather than D (Baldwin 1996). Such rapid refolding intermediates may be expected to show a large burst-phase refolding amplitude with a sigmoidal denaturant dependence. In contrast, InlB has a small burst-phase amplitude with a shallow linear urea dependence (Fig. 8). These observations do not support the formation of refolding intermediates, but instead support the two-state kinetic model.

A simple test for two-state kinetics is to compare equilibrium and two-state kinetic folding parameters. If the folding kinetics are two state, the thermodynamic parameters ($\Delta G^{\circ}_{u,H_2O}$ and *m*-value) determined from the ratio of folding and unfolding rate constants should match those determined from equilibrium measurements.[3] For InlB, $\Delta G^{\circ}_{u,H_2O}$ and *m*-values are within 0.1–0.2 kcal.mol^{-1} and 0.2–0.4 kcal.mol^{-1}.M^{-1} of equilibrium values, respectively (Table 1). The agreement between these kinetic and equilibrium parameters strongly supports a kinetic two-state mechanism for InlB folding.

Size of the folding transition state

Because of the simple two-state kinetic folding mechanism, the rate constant of folding of InlB can be used to directly infer structural features of the transition state ensemble. The Tanford beta value (β_T), which relates the urea dependence of the rate of folding to the equilibrium dependence (see Materials and Methods), provides an estimate of the degree of solvent accessibility of the transition state relative to the native state (Tanford 1968, 1970). The value of β_T for InlB is 0.40 (Table 1), suggesting that its folding transition state ensemble involves a little less than half of the protein. This value may reflect partial structure formation throughout the protein or complete structure formation in one region of the protein.

Comparison with other repeat proteins

Although exceptions exist, most helical repeat proteins have been found to fold in a thermodynamic, two-state transition, in which intermediate states are not populated at equilibrium (Tang et al. 1999; Zweifel and Barrick 2001; Mosavi et al. 2002; Lowe and Itzhaki 2007a). This result is surprising given the local topology and absence of long-range interactions characteristic of repeat proteins. It has been suggested that this high level of cooperativity arises from stabilizing interactions at the interfaces between energetically unstable repeats (Mello and Barrick 2004; Kajander et al. 2005). In contrast, two β-sheet-containing repeat proteins for which equilibrium folding studies have been reported, pertactin and pelC, show multistate equilibrium unfolding (Kamen et al. 2000; Junker et al. 2006).

[3]In this comparison, the kinetically determined $\Delta G^{\circ}_{u,H_2O}$ value must be corrected for the population of denatured state polypeptides with nonnative prolyl isomers. Here we used the relative amplitudes of the slow and fast refolding phases to estimate and correct for this population.

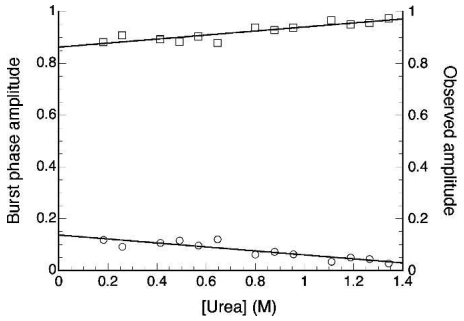

Figure 8. Fractional burst-phase amplitudes (circles) for refolding as a function of urea concentration in fluorescence-monitored experiments. Burst-phase amplitudes are calculated as the fractional difference between the observed and expected spectroscopic signal changes as determined by Equation 1. Total observed amplitudes ($1 - f_B$, squares) are the fraction of the expected signal change that is captured by the refolding progress curve.

The two-state equilibrium unfolding of InlB demonstrates that such behavior is not exclusive to helical repeat proteins, but can be maintained in β-sheet-containing LRRs. This behavior may reflect the fact that the elongated β-sheet structure of InlB involves interrepeat hydrogen bonding spanning all seven repeats, although such a structure is apparently not sufficient to impart two-state unfolding on pertactin and pelC. It is also quite likely that, like ankyrin and tetratricopeptide repeats, individual folded LRRs are very energetically unstable and are unlikely to populate folded conformations without docking to one another. This intrinsic instability decreases the likelihood of populating intermediates composed of only a few folded repeats at equilibrium, resulting in an all-or-none transition.

In contrast to the high degree of cooperativity revealed by equilibrium experiments, the kinetics of naturally occurring repeat proteins are much more complex, as evidenced by their multiple kinetic phases and nonlinear chevron plots (Tang et al. 1999; Zeeb et al. 2002; Mello et al. 2005). This complexity is consistent with on-pathway kinetic refolding and unfolding intermediates. Surprisingly, the folding kinetics of InlB conforms to a simple two-state mechanism. To our knowledge, InlB is the first naturally occurring repeat protein to be shown to possess such a simple kinetic mechanism.[4] It remains to be seen whether two-state kinetics is a general feature of LRR domains or whether it is specific to InlB. Irrespective of generality, InlB is an ideal candidate for further residue-specific analysis of its folding pathway via Φ-value analysis.

[4]Myotrophin, a four ankyrin repeat-containing protein, has been suggested to fold by a kinetic two-state mechanism with a moving transition state. However, a separate report from the same group invokes an on-pathway intermediate. As a result, the kinetic mechanism of this protein remains unclear (Lowe and Itzhaki 2007a,b).

Another common feature of repeat-protein folding is slow kinetics (Tang et al. 1999; Zeeb et al. 2002; Mello et al. 2005; Lowe and Itzhaki 2007a). Slow folding of repeat proteins is surprising because an empirical inverse relationship between relative contact order and folding rate predicts that repeat proteins should have very fast folding rates (Plaxco et al. 1998). InlB is no exception to this trend. With an extrapolated rate constant of 1.2 s^{-1} and a relative contact order of 4%, InlB folds approximately six orders of magnitude slower than predicted. It has been suggested that repeat proteins may fold slowly because two or more intrinsically unstable repeats must fold and subsequently dock together in the formation of the folding transition state (Mello and Barrick 2004; Kloss et al. 2007). A similar mechanism may limit the rate of folding of InlB, whose transition state buries approximately half its solvent-accessible surface area, based on the β_T-value determined here.

Materials and Methods

Protein expression and purification

The leucine-rich repeat domain and N-terminal capping motif of InlB were expressed from the plasmid pET28a (Novagen), a gift from the laboratories of Partho Ghosh and Pascale Cossart. The single cysteine in the leucine-rich repeat domain was replaced with a serine using the QuikChange Mutagenesis Kit (Stratagene) to avoid dimerization and promote long-term stability and reversible denaturation. InlB was expressed in *Escherichia coli* BL21 (DE3) cells by addition of 1 mM IPTG at $OD_{600} = 0.6$–0.8 for 4 h. Bacteria were lysed in 600 mM NaCl, 15 mM Tris (pH 8.0), 15 mM Imidazole and InlB was purified by Ni^{2+} chromatography, followed by a Sephacryl S-100 gel filtration column. Purified protein was dialyzed into 150 mM NaCl, 25 mM Tris (pH 8.0) and frozen at −80°C. Human cyclophilin was expressed in *E. coli* strain XA90 from the plasmid pHNJ, a gift from the laboratory of Dr. Christopher Walsh. Cyclophilin was expressed and purified as previously described (Liu et al. 1990; Mello et al. 2005).

Equilibrium folding studies

Ultrapure urea was purchased from Amresco. Urea was dissolved in water and treated with a mixed bed resin at a concentration of 5 g per 100 mL. Protein was denatured in 6–8 M urea, 25 mM Tris (pH 8.0), 150 mM NaCl, and titrated into a square 1-cm fluorescence cell containing native protein in 25 mM Tris (pH 8.0), 150 mM NaCl, using a Hamilton Microlab 500 titrator. Samples were equilibrated for 300 s at each urea concentration prior to signal acquisition. Urea-induced unfolding transitions were performed at 25°C and tracked by CD at 217 nm and by tryptophan fluorescence emission using a perpendicular 320-nm cutoff filter following excitation at 280 nm in an Aviv 62A DS Spectropolarimeter (Aviv Associates). Near-UV CD-monitored unfolding transitions were performed in the same way as described above in a J-810 spectropolarimeter (JASCO, Inc.). All equilibrium folding experiments were performed at 3 μM protein concentration.

Data were analyzed using the linear extrapolation method (Pace 1986; Bolen and Santoro 1988; Santoro and Bolen 1988), which assumes a linear relationship between the free energy of unfolding and urea concentration:

$$\Delta G^{\circ}(\text{urea}) = \Delta G^{\circ}_{u,H_2O} - m[\text{urea}] \quad (3)$$

Applying the standard relationship between reaction free energy and equilibrium constant yields the following equation:

$$K_U = K_{u,H_2O} \exp\ (-m_{urea}[\text{urea}]/\text{RT}) \quad (4)$$

A two-state model relates the observed signal (Y_{obs}), which is a population-weighted average of signals arising from the native and denatured states, to the unfolding equilibrium ($K_u = [D]/[N]$):

$$Y_{obs} = \mathrm{f}_N Y_N + f_D Y_D = (1/[1+K_U])\ Y_N + (K_U/[1+K_U])\ Y_D \quad (5)$$

where f_N and f_D are the fraction of native and denatured protein, respectively. Y_N and Y_D depend linearly on urea. For far-UV CD- and fluorescence-monitored transitions, Equation 5 was fitted to urea-induced denaturation curves to obtain $\Delta G^{\circ}_{u,H_2O}$ and *m*-values using the nonlinear least-squares analysis tool of Kaleidagraph 3.0 (Synergy Software). For near-UV CD spectra, global fitting was performed using the program Profit 6.0.0 (Quantum Soft) In the global fitting, a single $\Delta G^{\circ}_{u,H_2O}$ and *m*-value were assumed to describe unfolding at all wavelengths, whereas the baseline parameters were treated as wavelength-specific local parameters.

Analytical ultracentrifugation studies

Equilibrium analytical ultracentrifugation data were collected using a Beckman XL-A/XL-I ultracentrifuge (Beckman Coulter). Protein in 25 mM Tris (pH 8.0), 150 mM NaCl was dialyzed extensively at 4°C into the same buffer containing 0 mM, 10 mM, and 50 mM $CaCl_2$ prior to data collection. Protein concentrations ranged from ~8–45 μM. Samples were centrifuged at 25°C at 23,000, 26,000, and 30,000 rpm. Sedimentation equilibrium was established when concentration distributions, determined using absorbance optics, measured 2 h apart were coincident. Data were analyzed using the program SEDANAL (Stafford and Sherwood 2004).

Kinetic unfolding and refolding studies

Fluorescence-detected kinetic measurements of unfolding and refolding were made on an Applied Photophysics SX. 18MV-R stopped-flow fluorometer. Fluorescence changes were detected perpendicular to excitation at 280 nm using a 320-nm cutoff filter to monitor the changes in the environment surrounding the single tryptophan located in the third repeat of the LRR domain. Circular dichroism-detected kinetic measurements were made on a J-810 spectropolarimeter with a Bio-Logic SFM-20 rapid mixing stopped-flow attachment (JASCO, Inc.; Bio-Logic). CD changes were monitored at 217 nm. Final protein concentrations were typically 2–4 μM and 4–10 μM for stopped-flow fluorescence and CD, respectively. Samples contained 150 mM NaCl, 25 mM Tris (pH 8.0) and were at 25°C.

Amplitudes and rate constants for unfolding and refolding were determined using nonlinear least-squares analysis to fit the following equation to individual progress curves:

$$Y_{obs} = Y_{\infty} + \sum_{i=1}^{n} \Delta Y_i e^{-k_i t} \quad (6)$$

Y_{∞} represents the fluorescence or CD signal at equilibrium, ΔY_i represents the spectroscopic change contributed by the *i*th phase, and k_i represents the rate constant for the *i*th phase. Progress curves were considered to be best described by the minimum number of phases ($i = 1$, 2, or 3) that produced a satisfactory fit, based on distribution residuals and reduced χ^2 values.

The rate constants for refolding and unfolding were analyzed as a function of urea using a linear, kinetic two-state model, with the equation:

$$\log\ k_{\text{app}} = \log(k_{\text{f}} + k_{\text{u}}) = \log(k_{f,H_2O} 10^{m_f[urea]} + k_{u,H_2O} 10^{m_u[urea]}) \quad (7)$$

where m_f and m_u impart linear urea dependences on $\log k_f$ and $\log k_u$, respectively.

The Tanford beta value was calculated according to the following equation:

$$\beta_T = \frac{m_{eq}}{m_{kin}} \quad (8)$$

where m_{eq} is the slope of the dependence of the rate constant of the fast folding phase on urea concentration and m_{kin} is the kinetic *m*-value determined by fitting the chevron plot with a simple two-state model (Tanford 1968, 1970).

Acknowledgments

We thank Dr. Partho Ghosh and Dr. Pascale Cossart for providing us with the InlB clone, Dr. Christopher A. Walsh and C. Gary Marshall for providing a human cyclophilin expression construct, and Devon Sheppard for making the cysteine to serine substitution in the LRR domain of InlB. This work was supported by NIH grant GM68462, awarded to D.B.

References

Baldwin, R.L. 1996. On-pathway versus off-pathway folding intermediates. *Fold. Des.* **1:** R1–R8.

Banerjee, M., Copp, J., Vuga, D., Marino, M., Chapman, T., van der Geer, P., and Ghosh, P. 2004. GW domains of the *Listeria monocytogenes* invasion protein InlB are required for potentiation of Met activation. *Mol. Microbiol.* **52:** 257–271.

Bolen, D.W. and Santoro, M.M. 1988. Unfolding free energy changes determined by the linear extrapolation method. 2. Incorporation of ΔG degrees N-U values in a thermodynamic cycle. *Biochemistry* **27:** 8069–8074.

Bradley, C.M. and Barrick, D. 2005. Effect of multiple prolyl isomerization reactions on the stability and folding kinetics of the Notch ankyrin domain: Experiment and theory. *J. Mol. Biol.* **352:** 253–265.

Bradley, C.M. and Barrick, D. 2006. The Notch ankyrin domain folds via a discrete, centralized pathway. *Structure* **14:** 1303–1312.

Brandts, J.F., Halvorson, H.R., and Brennan, M. 1975. Consideration of the possibility that the slow step in protein denaturation reactions is due to *cis–trans* isomerism of proline residues. *Biochemistry* **14:** 4953–4963.

Ceulemans, H., De Maeyer, M., Stalmans, W., and Bollen, M. 1999. A capping domain for LRR protein interaction modules. *FEBS Lett.* **456:** 349–351.

Freiberg, A., Machner, M.P., Pfeil, W., Schubert, W.D., Heinz, D.W., and Seckler, R. 2004. Folding and stability of the leucine-rich repeat domain of internalin B from *Listeria monocytogenes*. *J. Mol. Biol.* **337:** 453–461.

Huyton, T. and Wolberger, C. 2007. The crystal structure of the tumor suppressor protein pp32 (Anp32a): Structural insights into Anp32 family of proteins. *Protein Sci.* **16:** 1308–1315.

Junker, M., Schuster, C.C., McDonnell, A.V., Sorg, K.A., Finn, M.C., Berger, B., and Clark, P.L. 2006. Pertactin β-helix folding mechanism suggests common themes for the secretion and folding of autotransporter proteins. *Proc. Natl. Acad. Sci.* **103:** 4918–4923.

Kajander, T., Cortajarena, A.L., Main, E.R., Mochrie, S.G., and Regan, L. 2005. A new folding paradigm for repeat proteins. *J. Am. Chem. Soc.* **127:** 10188–10190.

Kamen, D.E. and Woody, R.W. 2001. A partially folded intermediate conformation is induced in pectate lyase C by the addition of 8-anilino-1-naphthalenesulfonate (ANS). *Protein Sci.* **10:** 2123–2130.

Kamen, D.E., Griko, Y., and Woody, R.W. 2000. The stability, structural organization, and denaturation of pectate lyase C, a parallel β-helix protein. *Biochemistry* **39:** 15932–15943.

Kiefhaber, T., Kohler, H.H., and Schmid, F.X. 1992. Kinetic coupling between protein folding and prolyl isomerization. I. Theoretical models. *J. Mol. Biol.* **224:** 217–229.

Kim, H.M., Oh, S.C., Lim, K.J., Kasamatsu, J., Heo, J.Y., Park, B.S., Lee, H., Yoo, O.J., Kasahara, M., and Lee, J.O. 2007. Structural diversity of the hagfish variable lymphocyte receptors. *J. Biol. Chem.* **282:** 6726–6732.

Kloss, E., Courtemanche, N., and Barrick, D. 2007. Repeat protein folding: New insights into origins of cooperativity, stability, and topology. *Arch. Biochem. Biophys.* (in press). doi: 10.1016/j.abb.2007.08.03.4.

Kuwajima, K. 1989. The molten globule state as a clue for understanding the folding and cooperativity of globular-protein structure. *Proteins* **6:** 87–103.

Kuwajima, K., Garvey, E.P., Finn, B.E., Matthews, C.R., and Sugai, S. 1991. Transient intermediates in the folding of dihydrofolate reductase as detected by far-ultraviolet circular dichroism spectroscopy. *Biochemistry* **30:** 7693–7703.

Liu, J., Albers, M.W., Chen, C.M., Schreiber, S.L., and Walsh, C.T. 1990. Cloning, expression, and purification of human cyclophilin in *Escherichia coli* and assessment of the catalytic role of cysteines by site-directed mutagenesis. *Proc. Natl. Acad. Sci.* **87:** 2304–2308.

Lowe, A.R. and Itzhaki, L.S. 2007a. Biophysical characterisation of the small ankyrin repeat protein myotrophin. *J. Mol. Biol.* **365:** 1245–1255.

Lowe, A.R. and Itzhaki, L.S. 2007b. Rational redesign of the folding pathway of a modular protein. *Proc. Natl. Acad. Sci.* **104:** 2679–2684.

Mann, C.J. and Matthews, C.R. 1993. Structure and stability of an early folding intermediate of *Escherichia coli* trp aporepressor measured by far-UV stopped-flow circular dichroism and 8-anilino-1-naphthalene sulfonate binding. *Biochemistry* **32:** 5282–5290.

Marino, M., Braun, L., Cossart, P., and Ghosh, P. 1999. Structure of the lnlB leucine-rich repeats, a domain that triggers host cell invasion by the bacterial pathogen *L. monocytogenes*. *Mol. Cell* **4:** 1063–1072.

Mello, C.C. and Barrick, D. 2004. An experimentally determined protein folding energy landscape. *Proc. Natl. Acad. Sci.* **101:** 14102–14107.

Mello, C.C., Bradley, C.M., Tripp, K.W., and Barrick, D. 2005. Experimental characterization of the folding kinetics of the Notch ankyrin domain. *J. Mol. Biol.* **352:** 266–281.

Mosavi, L.K., Williams, S., and Peng, Z.Y. 2002. Equilibrium folding and stability of myotrophin: A model ankyrin repeat protein. *J. Mol. Biol.* **320:** 165–170.

Myers, J.K. and Oas, T.G. 2002. Mechanism of fast protein folding. *Annu. Rev. Biochem.* **71:** 783–815.

Myers, J.K., Pace, C.N., and Scholtz, J.M. 1995. Denaturant *m* values and heat capacity changes: Relation to changes in accessible surface areas of protein unfolding. *Protein Sci.* **4:** 2138–2148.

Pace, C.N. 1986. Determination and analysis of urea and guanidine hydrochloride denaturation curves. *Methods Enzymol.* **131:** 266–280.

Plaxco, K.W., Simons, K.T., and Baker, D. 1998. Contact order, transition state placement and the refolding rates of single domain proteins. *J. Mol. Biol.* **277:** 985–994.

Santoro, M.M. and Bolen, D.W. 1988. Unfolding free energy changes determined by the linear extrapolation method. 1. Unfolding of phenylmethanesulfonyl α-chymotrypsin using different denaturants. *Biochemistry* **27:** 8063–8068.

Schmid, F.X. 1992. Kinetics of unfolding and refolding of single-domain proteins. In *Protein folding*. (ed. T.E. Creighton), pp. 197–241. W.H. Freeman, New York.

Shastry, M.C. and Roder, H. 1998. Evidence for barrier-limited protein folding kinetics on the microsecond timescale. *Nat. Struct. Biol.* **5:** 385–392.

Stafford, W.F. and Sherwood, P.J. 2004. Analysis of heterologous interacting systems by sedimentation velocity: Curve fitting algorithms for estimation of sedimentation coefficients, equilibrium and kinetic constants. *Biophys. Chem.* **108:** 231–243.

Tanford, C. 1968. Protein denaturation. *Adv. Protein Chem.* **23:** 121–282.

Tanford, C. 1970. Protein denaturation. C. Theoretical models for the mechanism of denaturation. *Adv. Protein Chem.* **24:** 1–95.

Tang, K.S., Guralnick, B.J., Wang, W.K., Fersht, A.R., and Itzhaki, L.S. 1999. Stability and folding of the tumour suppressor protein p16. *J. Mol. Biol.* **285:** 1869–1886.

Wu, H., Maciejewski, M.W., Marintchev, A., Benashski, S.E., Mullen, G.P., and King, S.M. 2000. Solution structure of a dynein motor domain associated light chain. *Nat. Struct. Biol.* **7:** 575–579.

Zeeb, M., Rosner, H., Zeslawski, W., Canet, D., Holak, T.A., and Balbach, J. 2002. Protein folding and stability of human CDK inhibitor p19(INK4d). *J. Mol. Biol.* **315:** 447–457.

Zweifel, M.E. and Barrick, D. 2001. Studies of the ankyrin repeats of the *Drosophila melanogaster* Notch receptor. 2. Solution stability and cooperativity of unfolding. *Biochemistry* **40:** 14357–14367.